

Low-loss and directional output ZnO thin-film ridge waveguide random lasers with MgO capped layer

Clement Yuen, S. F. Yu,^{a)} Eunice S. P. Leong, H. Y. Yang, S. P. Lau, and N. S. Chen
*School of Electrical & Electronic Engineering, Nanyang Technological University, Block S2,
 Nanyang Avenue, Singapore 639798, Singapore*

H. H. Hng

School of Materials Engineering, Nanyang Technological University, Singapore, Singapore

(Received 28 July 2004; accepted 12 November 2004; published online 13 January 2005)

Room-temperature ultraviolet lasing characteristics of ZnO thin-film ridge-waveguide random lasers with MgO capped layer fabricated on *n*-type (100) Si substrate are reported. It is demonstrated that highly directional emission from the facets of the random lasers can be achieved. Reduction of scattering loss inside the random cavities can also be obtained. In addition, the improvement in the efficiency of the lasing characteristics of the random lasers by optical feedback is studied. © 2005 American Institute of Physics. [DOI: 10.1063/1.1850595]

Room-temperature UV random laser action has been demonstrated from randomly disordered ZnO polycrystalline thin films (i.e., irregular distribution of ZnO grains and voids) grown on Si substrate by laser ablation¹ or filtered cathodic vacuum arc (FCVA) technique.² The advantage of developing Si-based UV lasers using ZnO random cavities is to avoid the difficulty in cleaving smooth facets, thereby facilitating the mass production of low-cost UV lasing sources. However, high scattering loss and off-axial emission of random lasers limit their usefulness in most of the practical applications.³ In this letter, we proposed the use of annealed ZnO thin-film ridge waveguides with a MgO capped layer to realize random lasers with low scattering loss and directional optical output from the facets. The improvement in the efficiency of the lasing characteristics of the random lasers by optical feedback is also studied.

Figure 1(a) shows the schematic of the proposed ZnO thin-film ridge waveguide random laser. A SiO₂ buffer layer of thickness ~ 420 nm was formed on the surface of the *n*-type (100) Si substrate by thermal dry oxidation at 1000 °C for 10 h. Then, a ~ 200 -nm-thick ZnO film was deposited on the surface of the SiO₂ buffer layer by the FCVA technique.⁴ During the deposition, substrate temperature and oxygen partial pressure were set to 230 °C and 2×10^{-4} Torr, respectively. The random cavities were then formed inside the ZnO thin film by postgrowth annealing in open air at 900 °C for about 2 h.² Ridges of height, width, and separation of 100 nm, 2 μ m, and 500 μ m respectively, were subsequently formed on the surface of the annealed ZnO thin film by ion-beam sputtering. During the etching process, the chamber pressure, ion-beam current, ion-beam voltage, and flow rate of argon gas were set to be $\sim 1 \times 10^{-4}$ Torr, ~ 100 mA, 800 V, and ~ 14 sccm, respectively. The corresponding etching rate of the annealed ZnO was found to be ~ 12 nm/min. Figure 1(b) shows the scanning electron microscope (SEM) image of the ZnO ridge waveguide realized by ion-beam sputtering. It is shown that ion-beam sputtering is an effective way to etch the annealed ZnO thin films and the etching rate can be easily controlled by

varying the ion-beam current and voltage. Finally, a MgO capped layer of thickness ~ 200 nm was deposited on to the sample by the FCVA technique with the same conditions as that of ZnO.

Room-temperature UV lasing characteristics of the ZnO thin-film ridge-waveguide random lasers with and without MgO capped layer under optical excitation by a frequency-tripled Nd:YAG laser (at 355 nm) at pulsed operation (6 ns, 10 Hz) were studied. Optical pumping was achieved by using a cylindrical lens to focus a pump stripe of length L and width less than 8 μ m onto the ridge structure. Figure 2 shows the typical lasing characteristics of the samples with and without MgO capped layer with L set to 1 mm. From the unpolarized light–light curves given in Fig. 2(a), it is observed that a kink (i.e., pump threshold) occurs at ~ 0.61 MW/cm² (~ 0.69 MW/cm²) for the sample with (without) MgO capped layer. The increase in pump intensities above the pump threshold excites more sharp peaks, with

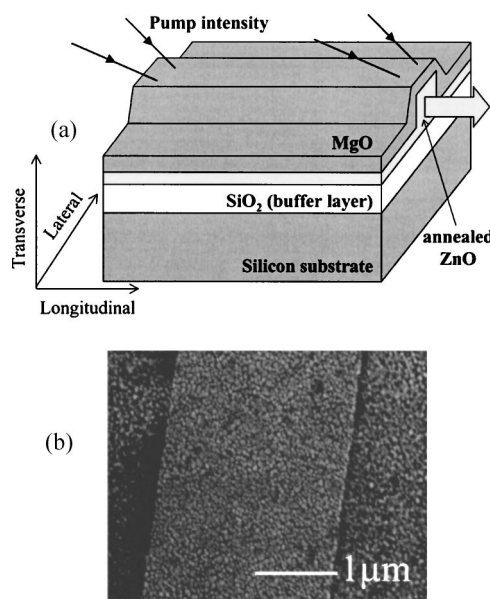


FIG. 1. (a) Schematic diagram of ZnO thin-film ridge waveguide random laser with a MgO capped layer. (b) SEM picture of the annealed ZnO thin film after etching a ridge structure by ion-beam sputtering.

^{a)} Author to whom correspondence should be addressed; electronic mail: esfyu@ntu.edu.sg

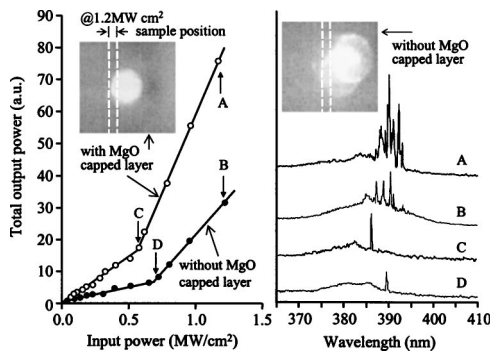


FIG. 2. (a) Light–light curves and (b) emission spectra of the samples with (○) and without (●) MgO capped layer measured at room temperature. The length of pump stripe L was set to 1 mm. The inset shows the TE emission far fields of the samples with and without MgO capped layer at pump intensity of 1.2 MW/cm². The dashed lines indicate the location of the sample.

linewidth less than 0.4 nm, as observed from the emission spectra in Fig. 2(b). Random lasing action is responsible for these observations because the facets are too rough to sustain round-trip conditions for Fabry–Perot-type lasing.² The reduction (increment) in pump threshold (output power) implies that the MgO capped layer has reduced the scattering loss of the random cavities. The polarization properties of the samples with MgO capped layer are similar to that given in Ref. 2 and hence, not elaborated herein. The TE-polarized far fields of the samples with and without the MgO capped layer at pump intensity of ~ 1.2 MW/cm² are also shown in the insets of Fig. 2. Light emitted from facet of the sample without MgO capped layer exhibits multiple circular spots. On the contrary, the sample with MgO capped layer shows a single bright-spot emission. Hence, it is shown that the annealed ZnO ridge waveguide random lasers with MgO capped layer can reduce scattering loss as well as realizing directional UV lasing output.

The improvement in lasing characteristics of the ZnO ridge waveguide random lasers can be explained by the trapping of scattering light inside the random cavities, as noted from Fig. 3.⁵ MgO capped layer traps the light scattered from the ZnO voids to the surface and to the side of the ridge waveguide by total internal reflection. Hence, light emitted from the facets is collimated to a single-spot profile and the scattering loss, α_{scat} , of the random cavities is also reduced.

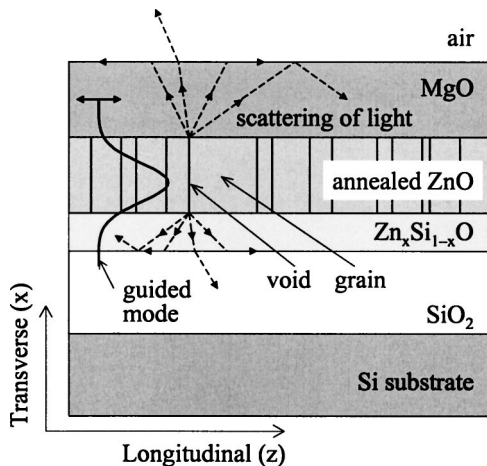


FIG. 3. Schematic cross section of the annealed ZnO ridge waveguide with MgO capped layer.

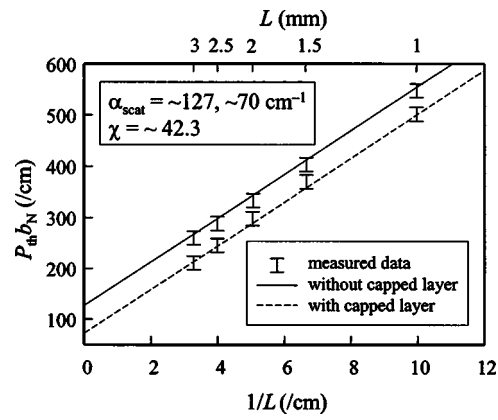


FIG. 4. Plots of $P_{\text{th}} b_N$ vs L^{-1} for the samples with (dashed line) and without (solid line) MgO capped layer where P_{th} was measured from the samples by varying L from 1 to 3 mm. $b_N = 0.77 \times 10^{-3} \text{ cm W}^{-1}$ is used in the plot.

The value of α_{scat} can be estimated from $g_{\text{th}} = \alpha_{\text{scat}} + f(L)$, where g_{th} is the threshold gain and $f(L)$ is the cavity loss of the random cavities. Based on the first-order approximation of one-dimensional random cavities,⁶ it is assumed that α_{scat} is independent of L and $f(L) \sim \chi L^{-1}$, where χ is defined as the normalized cavity loss. It is noted that by reducing χ , the pump threshold of the random lasers can be reduced. If the annealed ZnO film has a linear excitonic gain,⁷ that is $g_{\text{th}} = a_N(N_{\text{th}} - N_0) \approx a_N N_{\text{th}}$ where $a_N (= 2 \times 10^{-16} \text{ cm}^2)$ is the differential gain, N_{th} is the threshold carrier concentration, and N_0 is carrier concentration at transparency, g_{th} can be expressed in terms of the pump threshold P_{th} . From the carrier rate equation, we have $\eta P_{\text{th}} \lambda / d h c = N_{\text{th}} / \tau$ at threshold where $d (= 200 \text{ nm})$ is the thickness of ZnO film, $\tau (= 0.4 \text{ ns})$ is the carrier lifetime, $\lambda (= 355 \text{ nm})$ is the pump wavelength, h is the Planck's constant, c is the velocity of light, and $\eta (= 0.108)$ is the coupling efficiency. η is deduced by assuming only 87% of light is transmitted into the ZnO film, the ridge structure is exposed to 25% of the total excitation light and at most 50% of the pump power is converted to optical gain. Hence, it can be shown that $b_N P_{\text{th}} = \alpha_{\text{scat}} + \chi L^{-1}$ where $b_N = \eta a_N \tau \lambda / d h c$. Figure 4 plots $b_N P_{\text{th}}$ versus L^{-1} for samples with and without MgO capped layer. As P_{th} is deduced from the light–light curves manually (i.e., by interpolation), a small uncertainty of P_{th} is unavoidable. To take into consideration the error of P_{th} , the graph of $b_N P_{\text{th}}$ is plotted with 5% tolerance error bars (i.e., $b_N P_{\text{th}} \pm 10 \text{ cm}^{-1}$). In addition, two lines are linearly fitted to the data within the allowed tolerance and the difference in the gradients of the two lines is limited to a maximum of 1%. As a result, the values of α_{scat} for samples with and without MgO capped layer are found to be ~ 70 and $\sim 127 \text{ cm}^{-1}$, respectively, from the y intercept of Fig. 4. These deduced values of α_{scat} are reasonable as the measured waveguide loss of the ZnO ridge waveguides is $\sim 45 \text{ cm}^{-1}$.⁴ The reduction of α_{scat} by $\sim 57 \text{ cm}^{-1}$ is considered to be significant. In addition, the insignificant difference in the gradients between the two fitted lines indicates that the presence of MgO capped layer does not change the longitudinal resonant conditions of the samples. This is expected as the radiation fields are not in resonance with the longitudinal guided modes inside the random cavities. Hence, the independence of α_{scat} on L and the dependence of $f(L)$ on L previously assumed is justified. The observations also account for the choice of the values of the parameters used to estimate b_N .

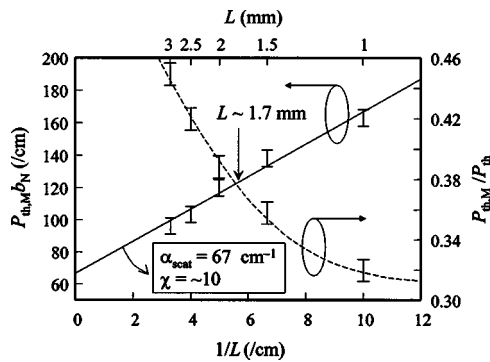


FIG. 5. Plots of $P_{th,M}b_N$ (solid line) and $P_{th,M}/P_{th}$ (dashed line) vs L^{-1} . The solid line is obtained from linear regression fitting within 5% tolerance (i.e., $b_N P_{th} \pm 5 \text{ cm}^{-1}$). $b_N = 0.77 \times 10^{-3} \text{ cm W}^{-1}$ is used in the plot.

To study the lasing characteristics of the random cavities under the influence of optical feedback, one cleaved facet of the sample with MgO capped layer was coated with a ~ 100 -nm-thick Al using an electron-beam evaporator. It is noted that the cavity loss of the Fabry–Perot cavity, which is superimposed to the random cavities by the presence of Al coating, is also proportional to L^{-1} such that the cavity loss of the Al coated samples will be approximately proportional to L^{-1} . The value of α_{scat} , which is mainly dependent on the geometry of the random cavities, will be less dependent on the optical feedback. Hence, the approximation $g_{th} = \alpha_{scat} + \chi L^{-1}$ still holds for the Al coated samples. Figure 5 plots $P_{th,M}b_N$ versus L^{-1} where $P_{th,M}$ is the pump threshold of the samples with Al coating. The solid line is obtained from the linear regression fitting of the measured $P_{th,M}$ with 5% tolerance. It is observed that the variation of $P_{th,M}$ is approximately proportional to L^{-1} . However, the value of α_{scat} ($\sim 67 \text{ cm}^{-1}$) is found to be slightly less than that obtained from Fig. 4. This may be due to the variation in the reflectivity of the Al coated facet arising from the uncontrollable cleaving process (facet roughness) of the samples. On the other hand, the reduction of χ from ~ 42 to ~ 10 indicates that the pump threshold of the random cavities can be reduced significantly by optical feedback. Figure 5 also shows the pump threshold ratio between samples with and without Al coating, $P_{th,M}/P_{th}$, versus L^{-1} . The decrease in $P_{th,M}/P_{th}$ with the decrease in L implies that re-injection of light can reduce pump threshold of short cavities more effectively but

too short a cavity length is not preferred. L of $\sim 1.7 \text{ mm}$ is the optimized length for both $P_{th,M}b_N$ and $P_{th,M}/P_{th}$. Our results, however, contradict the theoretical prediction (i.e., $P_{th,M}/P_{th}$ decreases with the increase in L).⁸ This is because the pump light of our samples has longer localization length than that of lasing modes and our pumping scheme excites lasing modes uniformly along the laser cavity. Hence, the re-injection of light will be coupled to the lasing modes near the coated facet more effectively and $P_{th,M}b_N$ decreases with the decrease in L .

In conclusion, we have solved the problems of high scattering loss and off-axial emission of ZnO thin-film random cavities. This can be achieved simply by the formation of ridge waveguide on the disordered ZnO thin films with MgO capped layer. Furthermore, it is found that the lasing characteristics of the random lasers can be improved effectively by optical feedback only at an optimized length. Hence, our proposed ZnO random lasers can achieve high-performance UV lasing, which is compatible with the conventional facet-emitted lasers. It is believed that the ZnO random lasers will be one of the most promising UV lasing sources to realize low-cost UV optoelectronics to be integrated with Si-based electronics.

This work was supported by the Agency for Science, Technology and Research of Singapore (Project No. 022-101-0033) and Nippon Sheet Glass Foundation.

¹H. Cao, Y. G. Zhao, X. Liu, E. W. Seeding, and R. P. H. Chang, Appl. Phys. Lett. **75**, 1213 (1999).

²S. F. Yu, Clement Yuen, S. P. Lau, and H. W. Lee, Appl. Phys. Lett. **84**, 3244 (2004).

³Newsbreaks, Laser Focus World **40**, 11 (2004).

⁴S. F. Yu, Clement Yuen, S. P. Lau, Y. G. Wang, H. W. Lee, and B. K. Tay, Appl. Phys. Lett. **83**, 4288 (2003).

⁵Our transmission electron microscopy analysis has verified that there is an intermediate $\text{Zn}_x\text{Si}_{1-x}\text{O}$ layer of thickness $\sim 100 \text{ nm}$ and refractive index lower than that of ZnO, formed between the ZnO and SiO_2 interface during the postgrowth annealing process. The presence of the intermediate layer can also reduce the scattering of light at the interface between ZnO and SiO_2 by total internal reflection.

⁶H. Cao, J. Y. Xu, Y. Ling, A. L. Burin, E. W. Seeling, X. Liu, and R. P. H. Chang, IEEE J. Sel. Top. Quantum Electron. **9**, 111 (2003).

⁷J. Ding, H. Jeon, T. Ishihara, M. Hagerott, and T. Yao, Phys. Rev. Lett. **69**, 1707 (1992).

⁸Y. Feng and K. I. Ueda, Phys. Rev. A **68**, 025803 (2003).